Print ISSN 1226-9751

Original Article

Characteristic MRI Findings of Spinal Metastases from Various Primary Cancers: Retrospective Study of Pathologically-Confirmed Cases

Chansik An, Young Han Lee, Sungjun Kim, Hee Woo Cho, Jin-Suck Suh, Ho-Taek Song

Department of Radiology and Research Institute of Radiological Science, Yonsei University College of Medicine, Seoul, Korea

Purpose : The purpose of this study was to find and categorize the various magnetic resonance imaging (MRI) findings of spinal metastases that correlate with the type of primary cancer.

Materials and Methods: We retrospectively reviewed gadolinium-enhanced magnetic resonance images of 30 patients with 169 spinal metastatic lesions from lung cancer (n = 56), breast cancer (n = 29), colorectal cancer (n = 20), hepatocellular carcinoma (HCC) (n = 17), and stomach cancer (n = 47). The size, location, extent of invasion, signal intensity, margin, enhancement pattern, and osteoblastic or osteolytic characteristics of each metastatic tumor were analyzed.

Results: The metastatic lesions from HCC were larger than those from the other primary tumors ($P < 0.05$) except for colorectal cancer ($P = 0.268$). Well-defined metastatic tumor margins were more frequently seen in lung cancer and breast cancer ($P < 0.01$). All but HCC showed a tendency to invade the vertebral body rather than the posterior elements ($P < 0.02$). Colorectal cancer and HCC showed a tendency toward extraosseous invasion without statistical significance. HCC showed a characteristic enhancement pattern of 'worms-in-a-bag'. Rim enhancement with a sclerotic center was only seen in spinal metastases from stomach cancer.

Conclusion: Despite many overlapping imaging features, spinal metastases of various primary tumors display some characteristic MRI findings that can help identify the primary cancer.

Index words : Spine · Magnetic resonance imaging · Metastasis

INTRODUCTION

The skeletal system is the third most common site for metastasis following the lung and the liver, and the spine is the most common site of skeletal metastasis regardless of the origin of primary cancer (1). Spinal metastases may be the initial presentation in 8–69% of patients (2). Carcinomas of the breast, prostate, and lung are well-known primary tumors which preferentially metastasize to the spine, and carcinomas from the thyroid, gastrointestinal (GI) tract, and kidney are also encountered at low rates (3, 4). However, in about 0.5–12.5% of spinal metastases, the primary site is not known at the initial diagnosis (5–8). Aside from detection and diagnosis of spinal metastasis, identifying the origin of the primary cancer is also critical because it can affect the treatment plan.

Magnetic resonance imaging (MRI) is widely used for screening for spinal metastasis in high-risk patients because of its superior diagnostic capability compared to other modalities such as scintigraphy, computed tomography (CT), and positron emission tomography (PET-CT) (9). MRI is also better at detecting epidural and bone marrow tumor infiltration and in delineating

• Received; July 17, 2012 • Revised; November 21, 2012
• Accepted; February 19, 2013
Corresponding author : Ho-Taek Song, M.D., Ph.D.
Department of Radiology, College of Medicine, Yonsei University, 50 Yonsei-ro, Seodaemun-gu, Seoul 120-752, Korea.
Tel. 82-2-2228-2370, Fax. 82-2-393-3035
E-mail : hotsong@yuhs.ac

the extraosseous soft tissue component of a neoplasm from the normal paraspinal soft tissue and neural structures (10–12). Therefore, understanding the characteristic MRI findings of spinal metastases from various primary tumors would be useful for both accurate diagnosis of spinal metastasis and identification of the origin of the primary cancer.

The purpose of this study was to find and categorize the various MRI findings of spinal metastasis according to the origin of primary cancer.

MATERIALS AND METHODS

Patients

Our institutional review board approved this retrospective study and waived the informed consent requirement. Sixty-six consecutive patients who had been reported as having spinal metastasis were subsequently confirmed by surgery or biopsy within one month after diagnosis between February 2007 and May 2010. Patients were excluded from the study if (1) MRI had not been performed within 30 days before surgery or biopsy (n=21), (2) the primary cancer remained unknown at the time of enrollment for this study (n=8), or (3) spinal metastasis from certain types of primary cancer because the number of metastatic lesions was too small (< 3 lesions for each type) (n=7, from cervical cancer, renal cell carcinoma, transitional cell carcinoma, prostate cancer, cholangiocellular carcinoma, and pancreatic adenocarcinoma). Overall, 169 spinal metastatic lesions in 30 patients were included in this study. Of these 30 patients, 14 were men with a mean age of 66 years (age range, 35–77) and 16 were women with a mean age of 58 years (age range, 30–74). In terms of the number of metastatic lesions associated with the various primary tumors, 7 patients had 56 spinal metastatic lesions from lung cancer, 6 had 29 lesions from breast cancer, 7 had 20 lesions from colorectal cancer, 7 had 17 lesions from hepatocellular carcinoma (HCC), and 3 had 47 lesions from stomach cancer. Although nearly every patient had multiple lesions, only one or two lesions were proved to be metastatic by surgery or biopsy. The remaining lesions were considered as having the same origin as the biopsy- or surgery-proven metastatic lesion.

MRI

The MRI studies were performed on 1.5-T (Intera Achieva 1.5 T, Philips Medical Systems, Best, The Netherlands) and 3.0-T MRI machines (Intera Achieva 3.0 T, Philips Medical Systems; or Trio a TIM, Siemens Medical Solutions, Erlangen, Germany) with the SENSE spine coil. All sequences were acquired with the patient lying supine. For cervical, thoracic, and lumbar spine MRI, T1-weighted spin-echo sagittal MRI (For 1.5-T, repetition time [TR] of 500–800 ms and echo time [TE] of 8–12 ms; For 3.0T, TR of 400–500 ms and TE of 8–10 ms) and T2-weighted spin-echo sagittal MRI (For 1.5-T, TR of 2000–3000 ms and TE of 60–120 ms; For 3.0-T, TR of 2000–2500 ms and TE of 8–10 ms) with/without fat suppression were used. For both T1-weighted and T2-weighted spin-echo sagittal MRI, slice thickness, intersection gap, matrix size, and field of view were 3–5 mm, 0.3–0.4 mm, 256–512 × 192–275, and 27–32 cm, respectively. The axial images of T1-weighted and T2-weighted spin echo MRI were obtained at the levels suspected to have metastatic lesions with slice thickness, intersection gap, TR and TE being 6–10 mm, 0.6–1.0 mm, 600–650 ms, and 8–10 ms for 1.5-T MR machine and 4–8 mm, 0.4–0.8 mm, 400–500 ms, and 7–8 ms for 3.0-T MR machine. Matrix size and field of view for axial images were 256× 256 and 23 cm with variations depending on patient size. All MRI protocols also included a T2-weighted sagittal whole spine view with the same TR and TE as T2-weighted spin-echo sagittal MRI. Contrast-enhanced T1-weighted spin-echo MRI with fat-suppression was performed in the sagittal plane followed by the axial plane after intravenous administration of 0.1 mmol/kg gadolinium-diethylenetriaminepentaacetic acid (Magnevist; Schering AG, Berlin, Germany).

Image Analysis

One of the authors (C.A.) reviewed the MR images to record the size, location, extent of invasion, signal intensity, margin, enhancement pattern, and osteoblastic or osteolytic characteristics of each metastatic tumor. In cases where the first author was not confident in his decision, another author (H.T.S. with 9 years of experience in musculoskeletal imaging) reviewed the MR images with the first radiologist (C.A.) to draw final conclusions by mutual consensus. The reviewers were aware of a diagnosis of spinal

metastasis but were unaware of the type of primary cancer or other clinical information. The maximum diameter of each tumor was measured in the sagittal plane. When a whole vertebral body was involved in metastasis (including cases of pathologic vertebral collapse) or a tumor invaded the posterior elements of a vertebra without mass formation, the size was not measured. For the location of each lesion, the vertebra was divided into two regions: the vertebral body and the posterior elements (pedicle, transverse process,

Table 1. The Margin, Signal Intensity, Location in a Vertebra, Extent of Invasion, and Enhancement Pattern of Metastatic Lesions According to the Origin of Primary Cancer

	Stomach cancer (n=47)	Colorectal cancer (n=20)	HCC (n=17)	Lung cancer (n=56)	Breast cancer (n=29)	Total (n=169)
Margin						
Well-defined	27/47 (57.4%)	10/20 (50%)	6/17 (35.3%)	44/56 (78.6%)	24/29 (82.8%)	111/169 (65.7%)
Ill-defined	20/47 (42.6%)	10/20 (50%)	11/17 (64.7%)	12/56 (21.4%)	5/29 (17.2%)	58/169 (34.3%)
P-value*	0.31	1	0.24	< 0.001	< 0.001	< 0.001
SI on T1-WI						
High	0/47 (0%)	0/20 (0%)	0/17 (0%)	16/56 (28.6%)	0/29 (0%)	16/169 (9.5%)
Iso-to low	47/47 (100%)	20/20 (100%)	17/17 (100%)	40/56 (71.4%)	29/29 (100%)	153/169 (90.5%)
P-value*	NA	NA	NA	< 0.001	NA	< 0.001
SI on T2-WI						
High	11/47 (23.4%)	17/20 (85%)	14/17 (82.4%)	35/56 (62.5%)	17/29 (58.6%)	94/169 (55.6%)
Iso-to low	36/47 (76.6%)	3/20 (15%)	3/17 (17.6%)	21/56 (37.5%)	12/29 (41.4%)	75/169 (44.4%)
P-value*	< 0.001	< 0.001	0.004	0.061	0.362	0.144
Location						
Vertebral body	43/47 (91.5%)	15/20 (75%)	6/17 (35.3%)	46/56 (82.1%)	26/29 (89.7%)	136/169 (80.5%)
Posterior elements	4/47 (8.5%)	5/20 (25%)	11/17 (64.7%)	10/56 (17.9%)	3/29 (9.3%)	33/169 (19.5%)
P-value*	< 0.001	0.02	0.24	< 0.001	< 0.001	< 0.001
Extent of Invasion						
Intraosseous	46/47 (97.9%)	9/20 (45%)	5/17 (29.4%)	43/56 (76.8%)	27/29 (93.1%)	130/169 (76.9%)
Extraosseous	1/47 (2.1%)	11/20 (55%)	12/17 (70.6%)	13/56 (23.2%)	2/29 (6.9%)	39/169 (23.1%)
P-value*	< 0.001	0.67	0.09	0.02	< 0.001	< 0.001
Enhancement Pattern						
Homogeneous	9/47 (19.1%)	1/20 (5%)	7/17 (41.2%)	18/44 (40.9%)†	6/10 (60%)†	41/169 (24.3%)
Heterogeneous	2/47 (4.3%)	17/20 (85%)	4/17 (23.5%)	26/44 (59.1%)†	4/10 (40%)†	53/169 (31.4%)
Non-enhancing	8/47 (17%)	2/20 (10%)	–	–	–	10/169 (5.9%)
Rim-enhancing	28/47 (59.6%)	–	–	–	–	28/169 (16.6%)
'Worms in a bag'	–	–	6/17 (35.3%)	–	–	6/169 (3.6%)
Non-applicable‡	–	–	–	12	19	31/169 (18.3%)

Note.— HCC = hepatocellular carcinoma, SI = signal intensity, NA = non-applicable. T1/T2-WI = T1/T2-weighted images

* One-sample T-test was performed to determine whether a certain type of primary cancer had a statistically significant tendency in terms of margin, signal intensity, location in a vertebra, and extent of invasion on MRI.

† After excluding non-applicable lesions from the total

‡ For these lesions, only non-enhanced MR images were present.

lamina, facet joint, and spinous process). When a tumor invaded body and posterior elements, the location of the tumor was classified based on the location of the epicenter of the tumor. The extent of tumor invasion was determined by classifying each lesion as an intraosseous or extraosseous lesion. Each tumor was categorized according to the margin (well-defined or ill-defined), signal intensity relative to the muscle nearby (hyperintense or iso- to hypointense), and enhancement pattern. A metastatic tumor was considered to have a well-defined margin if the tumor is distinctly separable from the adjacent normal tissue and has a smooth and regular outline. When the tumor did not satisfy these criteria or a whole vertebral body was involved, the margin of the tumor was considered ill-defined. The patterns of enhancement were classified as homogeneous, heterogeneous, non-enhancing, rim-enhancing, or worms-in-a-bag. We named the worms-in-a-bag pattern after the appearance of many strongly-enhancing curvilinear structures within a moderately-enhancing large mass. Whenever available, CT or PET-CT scan was used to determine whether a tumor was osteoblastic, osteolytic, or mixed.

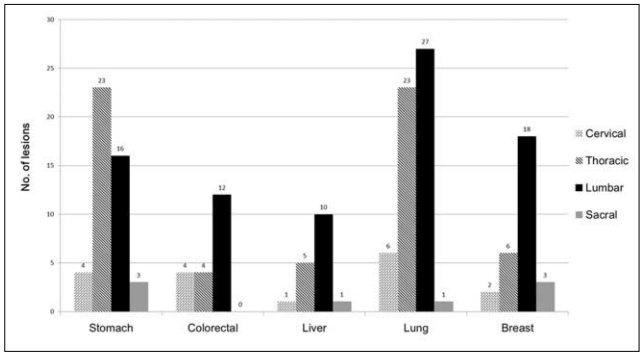

Fig. 1. Vertebral levels of spinal metastasis according to the origin of primary cancer.

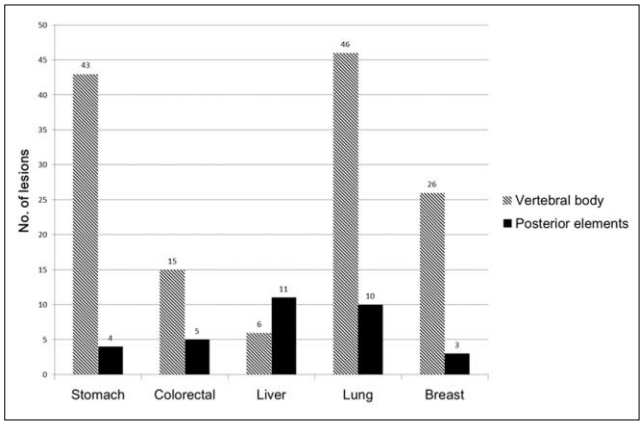

Fig. 2. Predilection for sites of metastasis according to the five different types of primary cancer.

Statistical Analysis

The Kruskal-Wallis test followed by a post-hoc

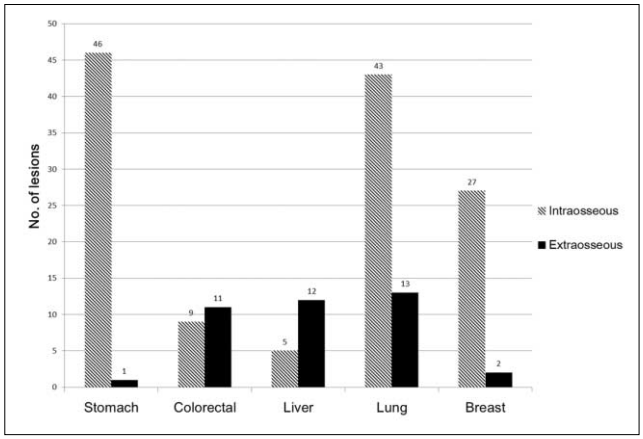

Fig. 3. Tendency toward intra- or extraosseous invasion of spinal metastasis according to the five different types of primary cancer.

Table 2. Osteolytic and Osteoblastic Characteristics of Spinal Metastases from Five Different Primary Tumors

	Osteoblastic	Osteolytic	Mixed	Indeterminate*	Total
Stomach cancer	21	6	20	0	47
Colorectal cancer	0	6	5	9	20
HCC	4	8	1	4	17
Lung cancer	4	24	8	20	56
Breast cancer	5	3	10	11	29
Total	33	43	44	44	169

Note.— HCC = hepatocellular carcinoma

* These indeterminate cases did not have reference images such as CT or PET-CT scans.

analysis using the Mann-Whitney test was used to determine whether there was a significant difference in size among the metastatic lesions originating from different primary tumors. Bonferroni correction was used for multiple comparisons. For tumor margin, signal intensity, predilection for a particular location within a vertebra, and tendency for intra- or extra-osseous invasion, one sample T-test was performed for each type of primary cancer to determine whether the ratios of well- to ill-defined margin, hyper- to iso- to hypo-intense, vertebral body to posterior elements, and intra- to extra-osseous invasion were significantly higher or lower than 0.5. The Chi-square test was used to determine the relationship between signal intensity on T2-weighted images and osteolytic or osteoblastic characteristics. A P-value less than 0.05 was considered to indicate a significant difference. All analyses used statistical software (PASW 18, Chicago, Illinois, USA).

RESULTS

Forty-two metastatic lesions were found to involve entire vertebral bodies. Eight lesions invaded the posterior elements of the vertebrae without forming expansible masses. The remaining 119 lesions ranged between 0.2 cm and 8 cm, with a mean of 1.4 cm in size. The mean tumor size was 1.12, 2.02, 3.43, 1.05, and 1.08 cm for stomach cancer, colorectal cancer, HCC, lung cancer, and breast cancer, respectively. Statistical analysis revealed a significant difference in size between the primary tumors ($P = 0.008$), and the metastatic lesions from HCC were larger than those from the other primary tumors ($P < 0.05$) except for colorectal cancer ($P = 0.268$).

The margin, signal intensity, location within a vertebra, extent of invasion, and enhancement pattern of metastatic lesions according to the origin of primary cancer are summarized in Table 1. A well-defined tumor margin was more frequently seen in spinal metastases from lung cancer and breast cancer ($P < 0.01$) than in those from the other primary tumors ($P > 0.24$ for all). Signal intensity was generally iso- to hypointense on T1-weighted images, as only 16 lesions (9.5%, 16 of 169, all from lung cancer) showed hyperintensity. However, signal intensity was variable on T2-weighted images, with slightly more than half

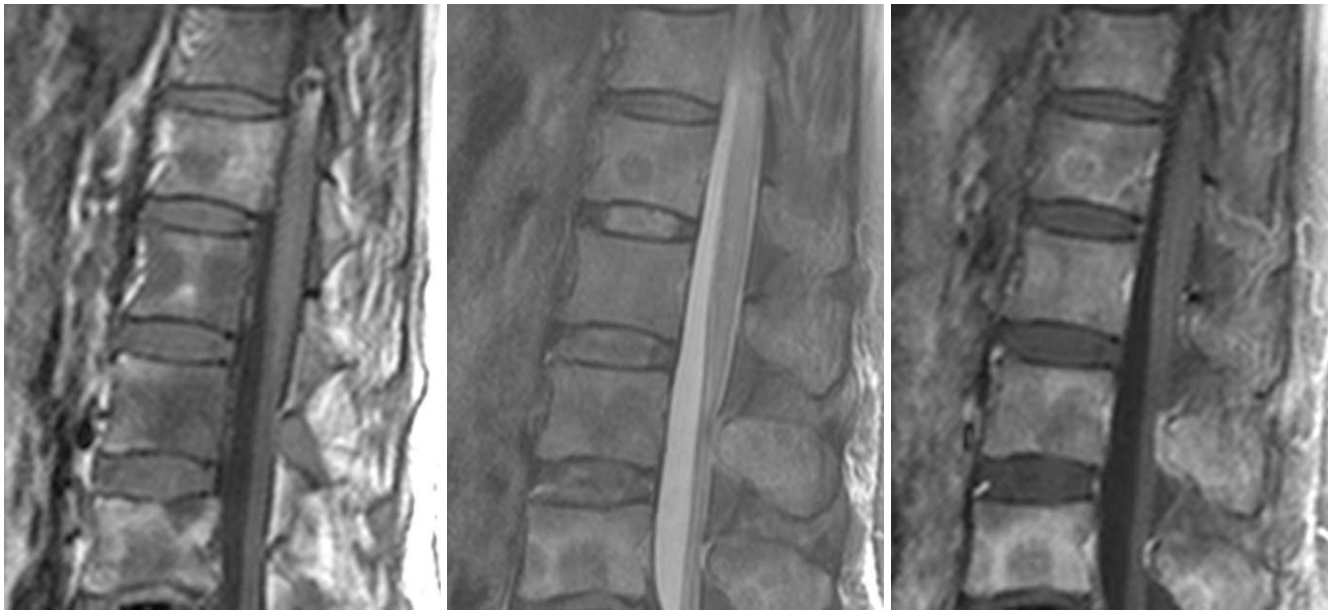

a b c

Fig. 4. A 60-year-old woman with advanced gastric cancer.

a. T1-weighted sagittal image of the thoracolumbar spine showing multiple hypointense metastatic lesions.

b. On fat-suppressed T2-weighted sagittal image, the lesions show hyperintensity in the periphery but hypointensity in the center, which may indicate sclerotic changes in the center of the metastatic lesions.

c. Contrast-enhanced T1-weighted sagittal image with fat suppression demonstrates enhancement in the periphery of the lesions as well as involvement of the bone marrow.

(55.6%, 94 of 169) showing hyperintensity: lesions from stomach cancer tended to show iso- to hypointensity; colorectal cancer and HCC showed hyperintensity; lung cancer and breast cancer showed no definite tendency. Eighty three of 169 tumors (49.1%) occurred in the lumbar vertebrae and 61 lesions (36.1%) were in the thoracic vertebrae, with the remaining 17 (10.1%) and 8 (4.7%) lesions in the cervical and sacral vertebrae, respectively. This trend was also observed within the individual groups of primary cancer with the exception of stomach cancer, in which thoracic involvement (50%) was slightly more frequent than lumbar involvement (34.8%) (Fig. 1). Within a vertebra, 80.5% (136 of 169) of metastatic lesions were centered in the vertebral body rather than the posterior elements. Statistical analysis confirmed this tendency in all types of primary cancer ($P<0.02$ for all) except HCC, in which metastatic lesions were centered in the posterior elements (64.7%) more frequently than in the vertebral bodies (35.3%) with a non-significant P-value ($P = 0.24$) (Fig. 2). According to the classification of each lesion into

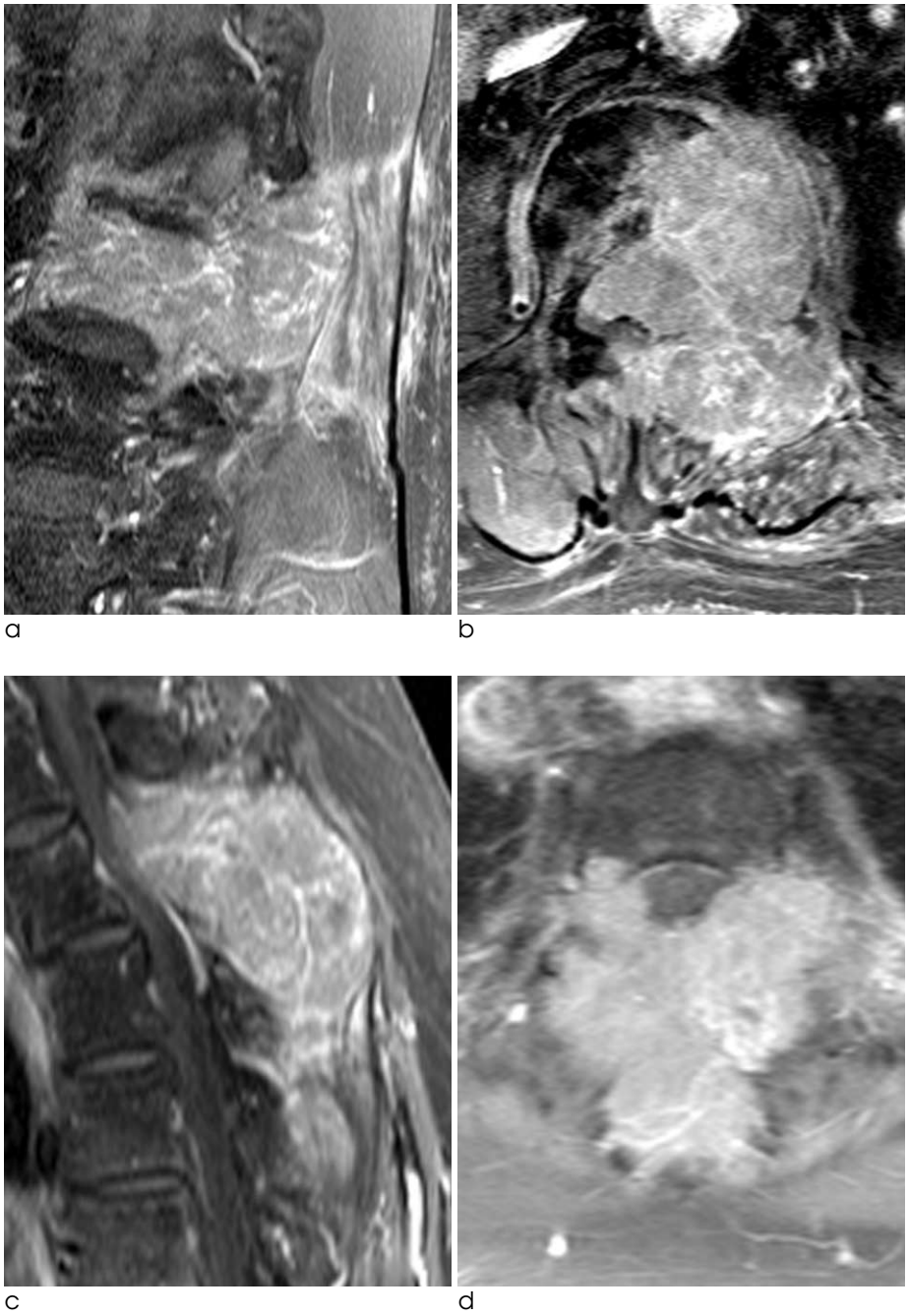

Fig. 5. Two patients with spine metastases from hepatocellular carcinoma.
a, b. Contrast-enhanced T1-weighted sagittal (**a**) and axial (**b**) images with fat-suppression of the lumbar spine of a 62-year-old man. A large expansile well-enhancing mass is invading the vertebral body and adjacent structures posteriorly, causing central canal obstruction. Note many curvilinear structures showing strong enhancement within the tumor ('worms-in-a-bag' enhancement pattern).
c, d. Contrast-enhanced T1-weighted sagittal (**c**) and axial (**d**) images with fat-suppression of the cervical spine of a 69-year-old woman. The location, extent of disease, and enhancement pattern are almost the same as those seen in the patient in **a, b.**

intra- or extraosseous invasion, spinal metastases from stomach cancer, lung cancer, and breast cancer tended to be confined to the vertebrae (P<0.02), while colorectal cancer (55%, 11 of 20) and HCC (70.6%, 12 of 17) showed a tendency toward extra-osseous invasion with non-significant P-values (P=0.67 for colorectal cancer and P=0.09 for HCC) (Fig. 3). More than half (59.6%, 28 of 47) of the metastatic lesions from stomach cancer showed rim enhancement with a hypovascular center (Fig. 4). Many of the metastatic lesions (35.3%, 6 of 17) from HCC also showed a characteristic enhancement pattern of worms-in-a-bag, especially when they formed large masses (Fig. 5). These two enhancement patterns (rim-enhancing and worms-in-a-bag) were not found in the other types of primary cancer.

Osteolytic or osteoblastic characteristics according to the different primary tumors are shown in Table 2. Of 169 lesions, 44 were unable to be evaluated due to the lack of reference images such as CT or PET-CT scans. There was an evident correlation between the osteolytic or osteoblastic characteristics and the signal intensity on T2-weighted images but not on T1-weighted images. Forty-four lesions were found to be both osteolytic and osteoblastic. After excluding these lesions, 33 of the remaining 76 lesions showed osteoblastic characteristics on CT or PET-CT, of which 84.5% (28 of 33) displayed iso- to hypointensity on T2-weighted images. In contrast, 86% (37 of 43) of osteolytic lesions showed hyperintensity on T2-weighted images (Table 3 and Fig. 6).

Table 3. The Relationship Between Osteolytic or Osteoblastic Characteristics and Signal Intensity on T2-weighted Images

	Signal intensity on T2-weighted MR images		
Characteristic	High	Low or intermediate	Total
Osteoblastic	5 (15.2%)	28 (84.8%)	33 (100%)
Osteolytic	37 (86%)	6 (14%)	43 (100%)

Note.— Chi-square test revealed a significant relationship ($p < 0.001$).

DISCUSSION

In the results of our study, metastatic lesions in the spine showed differences in signal intensity, size, margin, location within a vertebra, extent of invasion, enhancement pattern and osteoblastic or osteolytic characteristics depending on the primary tumor, while the distribution of the involved vertebral levels was consistent and independent of the site of primary cancer.

Overall, 85% of the spinal metastases were found in the thoracolumbar regions of the spine, and the cervical and sacral regions were involved in 15% of the cases, which is consistent with a previous report

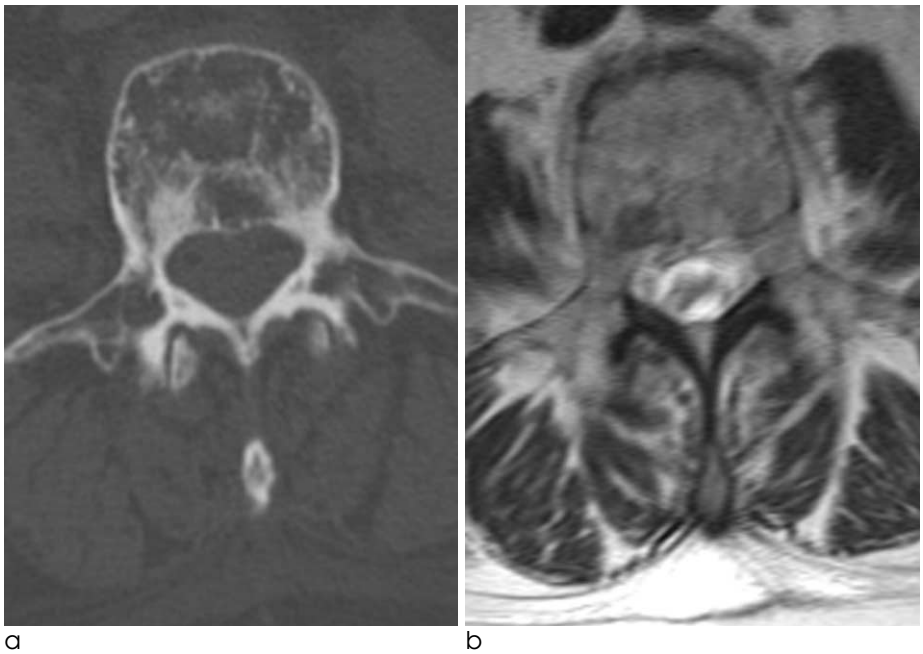

Fig. 6. A 56-year-old woman with spine metastases from breast cancer.
a. CT axial image shows mixed osteolytic and osteoblastic areas in the vertebra.
b. Corresponding T2-weighted axial image of the same level clearly demonstrates that sclerotic areas show hypointensity while osteolytic areas show hyperintensity on T2-weighted MRI.

(8). The signal intensity of spinal metastases was almost invariably iso- to hypointense on T1-weighted images but varied on T2-weighted images depending on the site of primary cancer. The variability of signal intensity on T2-weighted images is known to be related with osteoblastic or osteolytic characteristics (13), which is consistent with the results of the present study. The osteolytic lesions were more likely to be hyperintense and the osteoblastic lesions were more likely iso- to hypointense on T2-weighted images (Table 3), and this relationship was also seen in the individual groups of different primary tumors; stomach cancer tended to cause osteoblastic metastases with iso- to hypo-intensity on T2-weighted images, while colon cancer, lung cancer, and HCC tended to cause osteolytic metastases with hyperintensity on T2-weighted images. Furthermore, spinal metastases from breast cancer showed mixed characteristics in general, which was reflected in their variable signal intensities on T2-weighted images (Tables 1 and 2). However, osteoblastic or osteolytic characteristics are not sufficiently specific to identify the site of primary cancer because a patient with a certain type of cancer may have both osteoblastic and osteolytic lesions, and individual metastatic lesions can contain mixed components, as shown in the present study as well as in a previous study (4).

The size, margin, enhancement pattern, location within a vertebra, and extent of invasion (intraosseous or extraosseous) were significantly affected by the site of primary cancer. However, in order for these features to be used for identification of primary cancer site, the combinations of these findings should be considered rather than the individual findings. Tumor size and extent of invasion can be considered together; a larger size and extra-osseous invasion may represent the aggressiveness of the tumor. In this regard, spinal metastases from HCC and colorectal cancer showed aggressive behavior (Fig. 5 and Fig. 7). The aggressiveness of spinal metastases may also be reflected in the number of lesions per patient: 15 lesions per patient (47 lesions in 3 patients) with stomach cancer, 8 with lung cancer, 5 with breast cancer, 2.4 with HCC, and 2.8 with colorectal cancer, with a greater number of metastases signifying less aggressive disease given the number formed before detection. In the clinical

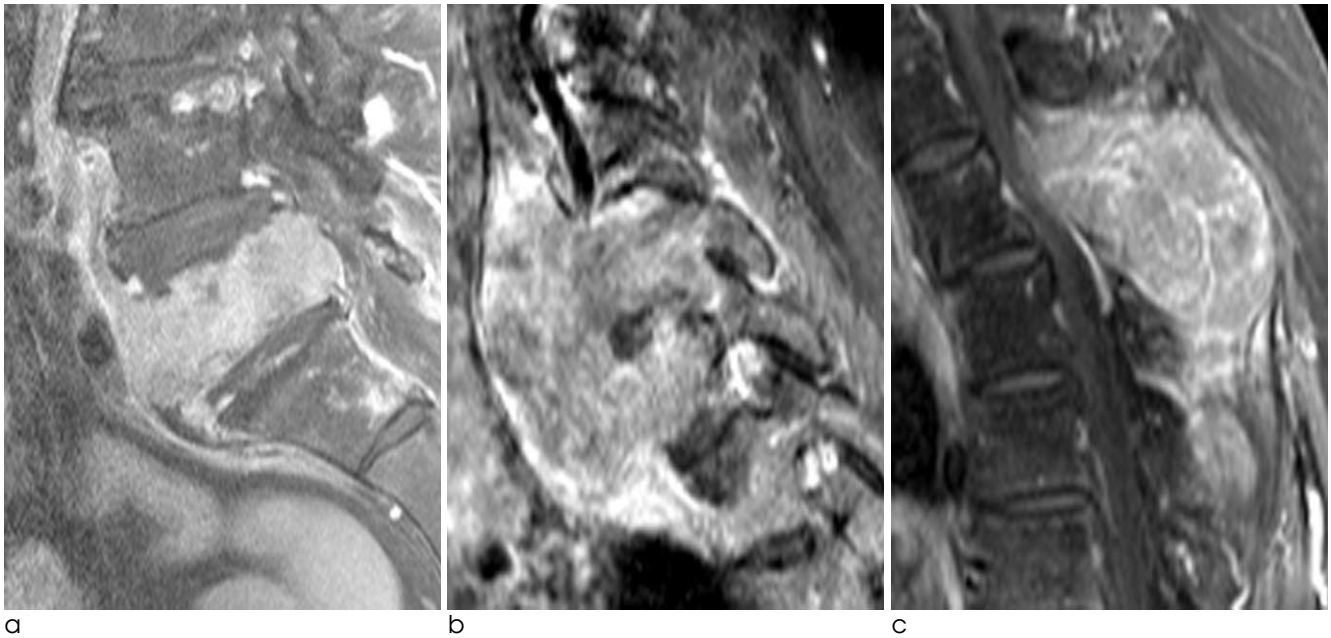

a b c

Fig. 7. Mass formation from spinal metastases of three different primary tumors.

a. A 76-year-old man with lung cancer. Contrast-enhanced T1-weighted sagittal image shows a homogeneously-enhancing metastatic mass replacing the 5th lumbar vertebra and spreading beneath the anterior longitudinal ligament upward.

b. A 74-year-old man with colorectal cancer. On contrast-enhanced T1-weighted sagittal image of the cervical spine, a heterogeneously-enhancing metastatic mass involving two vertebrae extends anteriorly to form a bulging mass.

c. A 69-year-old woman with HCC (same patient as in Fig. 5c). On contrast-enhanced T1-weighted sagittal image, a huge hypervascular mass invades the posterior aspect of the cervical spine. Note the 'worms-in-a-bag' enhancement pattern.

setting, this may imply that spinal metastases from HCC and colorectal cancer cause symptoms even when there are only a few spinal metastatic lesions, probably due to mass formation or extra-osseous invasion at a relatively early stage of disease. The differentiation factors between colorectal cancer and HCC were enhancement pattern and location within a vertebra; the worms-in-a-bag enhancement pattern and predilection for the posterior elements were only seen in spinal metastases from HCC. The other metastatic tumors rarely formed large masses, but the pattern was a little different; the metastatic mass from lung cancer or breast cancer spread along the anterior longitudinal ligament rather than forming a bulging mass (Fig. 7). In our data, 4 of 7 patients with HCC had at least one large expansile mass showing the worms-in-a-bag enhancement pattern with the epicenter being in the posterior elements. Although colorectal cancer also showed mass formation in 4 of 7 patients, it showed non-specific heterogeneous enhancement and no predilection for the posterior region (data not shown).

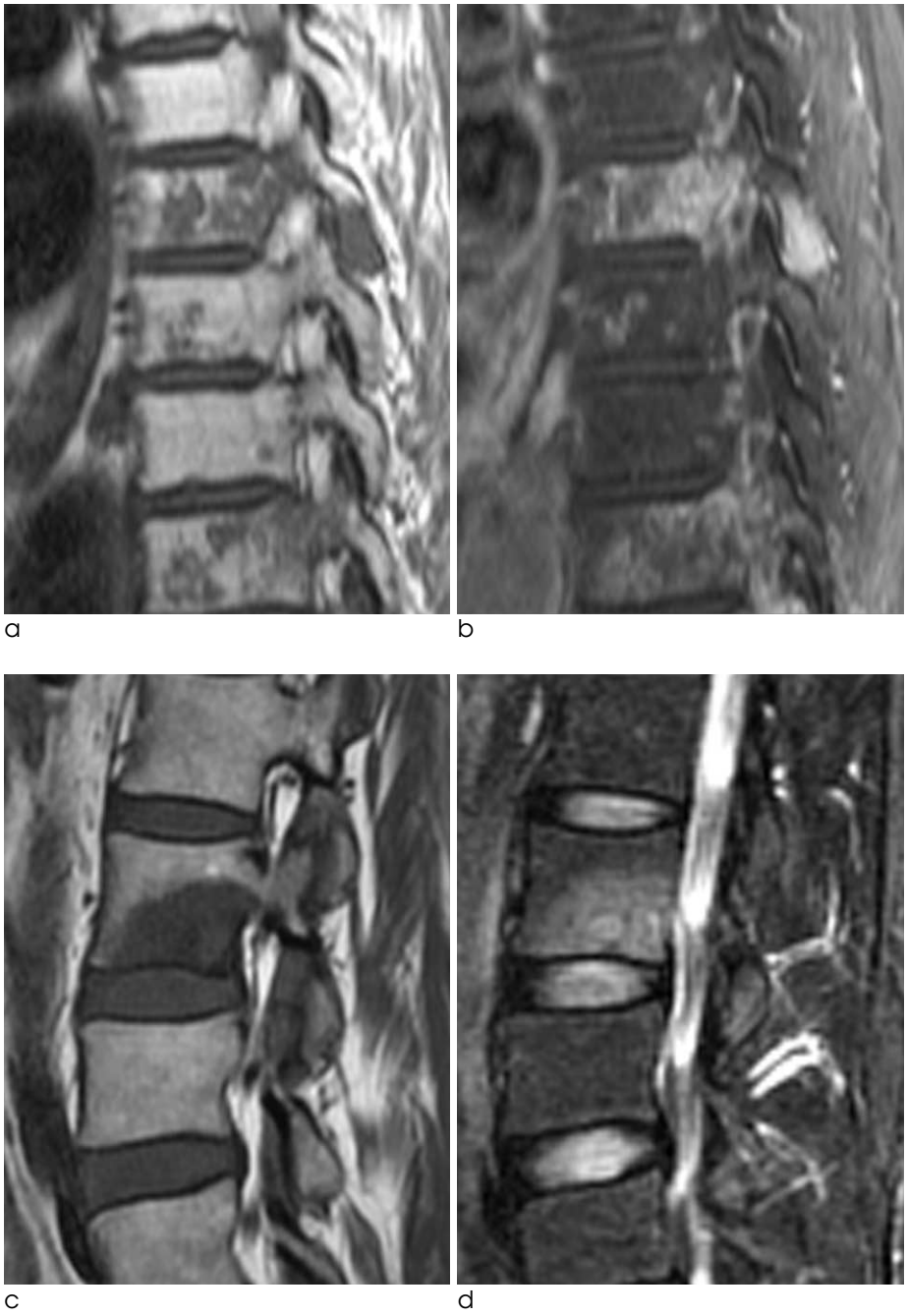

Fig. 8. Metastatic lesions confined to the vertebrae.
a, b. Pre-contrast (**a**) and contrast-enhanced with fat suppression (**b**) T1-weighted sagittal images of a 56-year-old woman with lung cancer. There are numerous well-defined hypointense lesions with non-specific heterogeneous contrast enhancement in the thoracic spine. These lesions are confined in the vertebrae, some of which appear to coalesce.
c, d. T1-weighted (**c**) and T2-weighted with fat suppression (**d**) sagittal images of a 45-year-old woman with breast cancer. There is a well-defined hypointense metastatic lesion with homogeneous enhancement in the lumbar vertebra. This lesion is also confined in the vertebral body without extraosseous invasion, despite its relatively large size.

Previous studies on spinal metastases from HCC mostly focused on clinical aspects. There have been few studies including radiologic findings of extrahepatic metastases from HCC (14–17). One of these studies only contains one case of spinal metastasis which shows a large heterogeneous lobulated destructive soft-tissue invading the posterior elements and adjacent structures (15). Another study reported that 55% (47 out of 85) of HCC patients with spinal metastasis presented with soft tissue formation (17). To our knowledge, however, no study has investigated on specific enhancement pattern of metastatic tumors from HCC, making our study the first to report the possibly specific enhancement pattern. A possible explanation for the worms-in-a-bag enhancement pattern might be a combination of hypervascularity of primary cancer and soft tissue formation. Thus, the combination of these four findings (large size, extraosseous invasion, predilection for the posterior elements, and worms-in-a-bag enhancement) may be characteristic of spinal metastasis from HCC.

In contrast to colorectal cancer and HCC, lung cancer, breast cancer, and stomach cancer tended to be confined to the vertebral bodies even when multiple (i.e., more than 10) lesions were present in one patient, which is probably the reason that the mean size of metastatic lesions was smaller in these primary tumors (Fig. 8). The rim-like enhancement with a non-enhancing center was noted only in spinal metastases from stomach cancer. The hypovascular area in the center showed hypointensity on both T1- and T2-weighted images, indicative of its sclerotic nature (Fig. 4). Spinal metastases from lung cancer and breast cancer showed a stronger tendency toward having a well-defined border than those from the other primary tumors, but this is not a specific finding because the other primary tumors except colorectal cancer were also more likely to form well-defined metastatic lesions (Table 1).

This study has several limitations. One limitation is a relatively smaller number of subjects than previous studies. Due to this small number of study subjects, it was not possible to evaluate many potentially important factors including tumor/node stage, histologic grade, or cell type, which could affect the MRI findings of spinal metastases even from the same primary cancer. In order to determine whether these factors are independent factors, the sample size of each primary cancer group has to be much larger than in this study. A small number of samples also led to an exaggeration of bias from clustered data, which is inevitable in studies of multiple metastatic lesions in the spine. In other words, multiple lesions within the same patient tend to have the same intrinsic characteristics in many aspects such as signal intensity, tumor margin, and enhancement pattern. However, the two unique enhancement patterns discovered in our study may be potentially specific findings because they were found exclusively in HCC (worms-in-a-bag) or stomach cancer (rim enhancement with a sclerotic center). Another limitation is that other primary tumors known to be prone to metastasize to the spine such as prostate cancer and thyroid cancer were not included in the study because bone metastasis is rarely confirmed by biopsy or surgery for these primary tumors in our institution. Lastly, the patients in our study were at different stages of their diseases, which may have affected the MRI findings.

In conclusion, despite having many overlapping imaging features, spinal metastases of various primary tumors display some characteristic MRI findings that can help identify the primary cancer. Specifically in our cases, colorectal cancer and HCC tended to form large masses at a relatively early phase of spinal metastasis. HCC often showed a distinctive radiological feature characterized by the formation of a large expansile mass in the posterior region with a worms-in-a-bag enhancement pattern, and rim enhancement with a sclerotic center was only seen in spinal metastases from stomach cancer.

Acknowledgements:

This study was supported by a grant from the Korean Health Technology R&D Project, Ministry of Health & Welfare, Republic of Korea (A110035).

References

1. Boland PJ, Lane JM, Sundaresan N. Metastatic disease of the spine. Clin Orthop Relat Res 1982;169:95-102
2. Schiff D, O'Neill BP, Suman VJ. Spinal epidural metastasis as the initial manifestation of malignancy: clinical features and diagnostic approach. Neurology 1997;49:452-456
3. Berrettoni BA, Carter JR. Mechanisms of cancer metastasis to bone. J Bone Joint Surg Am. American volume 1986;68:308-312
4. Guillevin R, Vallee JN, Lafitte F, Menuel C, Duverneuil NM, Chiras J. Spine metastasis imaging: review of the literature. J

Neuroradiol 2007;34:311-321
5. Daugaard G. Unknown primary tumours. Cancer Treat Rev 1994;20:119-147
6. Abbruzzese JL, Abbruzzese MC, Hess KR, Raber MN, Lenzi R, Frost P. Unknown primary carcinoma: natural history and prognostic factors in 657 consecutive patients. J Clin Oncol 1994;12:1272-1280
7. Katagiri H, Takahashi M, Inagaki J, Sugiura H, Ito S, Iwata H. Determining the site of the primary cancer in patients with skeletal metastasis of unknown origin: a retrospective study. Cancer 1999;86:533-537
8. Brihaye J, Ectors P, Lemort M, Van Houtte P. The management of spinal epidural metastases. Adv Tech Stand Neurosurg 1988;16:121-176
9. Ghanem N, Uhl M, Brink I, et al. Diagnostic value of MRI in comparison to scintigraphy, PET, MS-CT and PET/CT for the detection of metastases of bone. Eur J Radiol 2005;55:41-55
10. Chiewvit P, Danchaivijitr N, Sirivitmaitrie K, Chiewvit S, Thephamongkhol K. Does magnetic resonance imaging give value-added than bone scintigraphy in the detection of vertebral metastasis? Chot Mai Het Thang Phaet 2009;92:818-829
11. Beltran J, Noto AM, Chakeres DW, Christoforidis AJ. Tumors of the osseous spine: staging with MR imaging versus CT. Radiology 1987;162:565-569
12. Keogh C, Bergin D, Brennan D, Eustace S. MR imaging of bone tumors of the cervical spine. Magn Reson Imaging Clin N Am 2000;8:513-528
13. Ross JS, Moore KR, Borg B, Crim J, Shah LM. Diagnostic imaging: Spine. 2nd ed. Salt Lake City: Amirsys, 2010
14. Sugimura K, Kajitani A, Okizuka H, Sugihara M, Mizutani M, Ishida T. Assessing response to therapy of spinal metastases with gadolinium-enhanced MR imaging. J Magn Reson Imaging 1991;1:481-484
15. Sneag DB, Krajewski K, Giardino A, et al. Extrahepatic spread of hepatocellular carcinoma: spectrum of imaging findings. AJR Am J Roentgenol 2011;197:W658-664
16. Katyal S, Oliver JH, 3rd, Peterson MS, Ferris JV, Carr BS, Baron RL. Extrahepatic metastases of hepatocellular carcinoma. Radiology 2000;216:698-703
17. Seo HJ, Choi YJ, Kim HJ, et al. Evaluation of bone metastasis from hepatocellular carcinoma using 18F-FDG PET/CT and 99mTc-HDP bone scintigraphy: characteristics of soft tissue formation. Nuclear Medicine and Molecular Imaging 2011;45: 203-211

대한자기공명의과학회지 17:8-18(2013)

다양한 원발성 암의 척추전이 병변의 특징적인 자기공명영상 소견들: 병리학적으로 확인된 병변들의 후향적인 분석

[1]연세대학교 의과대학 세브란스병원 영상의학과

안찬식 · 이영한 · 김성준 · 조희우 · 서진석 · 송호택

목적: 척추전이의 자기공명영상 소견들 중 특정 원발성 암에 특이적인 소견들이 있는지 알아보고자 한다.
대상과 방법: 본 연구에서는 자기공명영상을 시행한 총 169개의 척추전이암 병변들 (56개는 폐암, 29개는 유방암, 20개는 대장암, 17개는 간세포암, 그리고 47개는 위암으로부터 기원)을 후향적으로 분석하였다. 각 병변의 크기, 위치, 침범 정도, 신호강도, 경계, 조영증강 양상, 그리고 골융해/골경화 특성들을 분석하여 원발성 암의 기원에 따라 차이가 있는지 보았다.
결과: 간세포암의 전이 병변들은 대장암을 제외하고는 (P=0.268) 다른 암에 비하여 크기가 유의하게 컸다 (P 〈 0.05). 경계가 좋은 병변은 폐암과 유방암에서 기원한 경우에서 더 흔히 관찰되었다 (P 〈 0.01). 간세포암을 제외한 모든 암에서 전이를 할 때 척추의 후부요소보다 척추체를 더 자주 침범하였다(P 〈 0.02). 대장암과 간세포암은 골외 침범을 더 자주 보였으나 통계학적 의미는 없었다 (P 〉 0.05). 간세포암과 위암의 전이병변들은 특징적인 조영증강 양상을 보였다.
결론: 일부 자기공명영상 소견들은 척추전이 병변이 어떤 원발성 암에서 기원한 것이지 예측하는 데 도움이 될 수 있다.

통신저자 : 송호택, (120-752) 서울시 서대문구 연세로 50, 연세대학교 의과대학 세브란스병원 영상의학과
Tel. (02) 2228-2370 Fax. (02) 393-3035 E-mail: hotsong@yuhs.ac